



HAL
open science

Logical modelling of myelofibrotic microenvironment predicts dysregulated progenitor stem cell crosstalk

Stephen Chapman, Estelle Duprez, Elisabeth Remy

► To cite this version:

Stephen Chapman, Estelle Duprez, Elisabeth Remy. Logical modelling of myelofibrotic microenvironment predicts dysregulated progenitor stem cell crosstalk. *BioSystems*, 2023, 231, pp.104961. <10.1016/j.biosystems.2023.104961>. <hal-04762151>

HAL Id: hal-04762151

<https://hal.science/hal-04762151v1>

Submitted on 31 Oct 2024

HAL is a multi-disciplinary open access archive for the deposit and dissemination of scientific research documents, whether they are published or not. The documents may come from teaching and research institutions in France or abroad, or from public or private research centers.

L'archive ouverte pluridisciplinaire **HAL**, est destinée au dépôt et à la diffusion de documents scientifiques de niveau recherche, publiés ou non, émanant des établissements d'enseignement et de recherche français ou étrangers, des laboratoires publics ou privés.



HAL Authorization

1 Logical modelling of myelofibrotic microenvironment predicts 2 dysregulated progenitor stem cell crosstalk

3

4

5

6 Chapman S. P. ¹, Duprez E. ², and Remy, E. ^{1*}

7

8 ¹ I2M, Aix-Marseille University, CNRS, Marseille, France

9 ² Epigenetic Factors in Normal and Malignant Haematopoiesis Lab., CRCM, CNRS, INSERM, Institut Paoli
10 Calmettes, Aix Marseille University, 13009 Marseille, France

11

12 Abstract

13 Primary myelofibrosis is an untreatable age-related disorder of haematopoiesis in which
14 a break in the crosstalk between progenitor Haematopoietic Stem Cells (HSCs) and
15 neighbouring mesenchymal stem cells causes HSCs to rapidly proliferate and migrate out
16 of the bone marrow. Around 90% of patients harbour mutations in driver genes that all
17 converge to overactivate hematopoietic JAK-STAT signalling, which is thought to be
18 critical for disease progression, as well as microenvironment modification induced by
19 chronic inflammation. The trigger to the initial event is unknown but dysregulated
20 thrombopoietin (TPO) and Toll-Like Receptor (TLR) signalling are hypothesised to initiate
21 chronic inflammation which then disrupts stem cell crosstalk. Using a systems biology
22 approach, we have constructed an intercellular logical model that captures JAK-STAT
23 signalling and key crosstalk channels between haematopoietic and mesenchymal stem
24 cells. The aim of the model is to decipher how TPO and TLR stimulation can perturb the
25 bone marrow microenvironment and dysregulate stem cell crosstalk. The model predicted

1

26 conditions in which the disease was averted and established for both wildtype and
27 ectopically JAK mutated simulations. The presence of TPO and TLR are both required to
28 disturb stem cell crosstalk and result in the disease for wildtype. TLR signalling alone was
29 sufficient to perturb the crosstalk and drive disease progression for JAK mutated
30 simulations. Furthermore, the model predicts probabilities of disease onset for wildtype
31 simulations that match clinical data. These predictions might explain why patients who
32 test negative for the JAK mutation can still be diagnosed with PMF, in which continual
33 exposure to TPO and TLR receptor activation may trigger the initial inflammatory event
34 that perturbs the bone marrow microenvironment and induce disease onset.

35

36 Keywords

37 Logical model, myelofibrosis, haematopoiesis, bone marrow, cell crosstalk

38

39 Introduction

40 Primary myelofibrosis (PMF) is an idiopathic age-related clonal neoplastic disorder of
41 haematopoiesis. Out of all the subsets of myeloproliferative neoplasms (including
42 polycythaemia and essential thrombocytosis), PMF represents the highest morbidity and
43 mortality and mean survival is estimated at less than 6 years post-prognosis (Bartalucci
44 *et al.* 2013; Bartels *et al.* 2020).

45 More than 90% of myelofibrosis cases harbour somatic mutations in the driver genes
46 JAK, CALR, or MPL that lead to constitutive activation of the JAK-STAT signalling
47 pathways (Coltro *et al.* 2021). Following JAK activation, haematopoietic stem cells
48 (HSCs) become hypersensitive to growth factors, rapidly proliferate and migrate from the
49 bone marrow (BM) to sites of extramedullary haematopoiesis in the liver and spleen
50 (Desterke *et al.* 2015; Hasselbalch. 2013). PMF is also accompanied by an event of
51 chronic inflammation, which appears to be secondary considering that independent
52 overexpression of each of the driver mutations in mice have been shown to recapitulate
53 distinctive features of human disease mutations leading to JAK overactivity (Rumi *et al.*,
54 2020).

55 Research has linked abnormally high levels of TGF β , a potent inflammatory cytokine
56 produced from atypical and dysmorphic megakaryocytes (MK) (Malara *et al.* 2018) in
57 response to disrupted thrombopoietin (TPO) signalling in both patients and mouse models
58 of the disease (Chagraoui *et al.* 2002; Melo-Cardenas *et al.* 2021). TPO, secreted from
59 fibroblasts, is essential for MK differentiation and maintenance of HSCs (Cui *et al.* 2021)
60 and signals through the JAK receptor (Varghese *et al.* 2017).

61 Current treatment protocols aim to disrupt the overactive STAT pathways (Stark and
62 Darnell Jr. 2012; Pardanani *et al.* 2011) and diminish the effects of chronic inflammation
63 but are unable to influence the altered BM (Kuykendall *et al.* 2020). Within the BM
64 microenvironment, HSCs reside in an endosteal niche and are engaged in constant
65 crosstalk with neighbouring Mesenchymal Stem Cells (MSCs). MSCs secrete the
66 chemokines CXCL12 and Vascular Cell Adhesion molecule-1 (VCAM1) which bind to
67 their respective receptors, CXCR4 and VLA4, expressed upon the surface of HSCs.

68 (Lubkova *et al.* 2011; Liekens *et al.* 2010). Chronic inflammation is believed to result in a
69 break in any of these communication pathways which then leads to HSC migration
70 (Caocci *et al.* 2017).

71 ligand-activated stimulation of Toll-Like Receptors (TLRs) are well documented to induce
72 chronic inflammation (Desterke *et al.* 2015; Fisher *et al.* 2017; Fisher *et al.* 2019; Fisher
73 *et al.* 2021; Mascarenhas *et al.* 2022), leading to the hypothesis that unregulated TLR,
74 and/or TPO signalling could be responsible for triggering chronic inflammation. This would
75 then perturb the BM microenvironment and disrupt the crosstalk between HSCs and
76 MSCs and lead to HSC migration and disease development. (Desterke *et al.* 2015). This
77 hypothesis emphasises a major role of the microenvironment in the development of
78 myeloproliferative neoplasms and is interesting to consider in the context of patients who
79 are “triple-negative” for one of the driver mutations (Tefferi and Vannucchi 2017), and for
80 the 0.1 – 0.2% of the general population who carry the JAK mutation without showing
81 overt signs of any myeloproliferative neoplasm (Nielsen *et al.* 2014).

82 It is well known that the presence of feedback circuits (or feedback loops) within biological
83 systems ensures the maintenance of dynamical stability (Cornish-Bowden and Cárdenas.
84 2008; Qian and Beard. 2006). The idiopathic onset of PMF is believed to arise from an
85 altered microenvironment that perturbs such feedback loops and results in disrupted
86 communication between progenitor stem cells residing within the BM. The challenge of
87 understanding disease onset, therefore requires a thorough understanding of how
88 regulatory circuits control and regulate HSC-MSK crosstalk, and this challenge can be
89 met using a computational systems approach. Construction of a computational model will

90 allow for a better understanding of the cause and effect of feedback loops and also
91 provides a tool for making *in silico* predictions.

92 Quantitative and qualitative mathematical modelling formalisms have become powerful
93 tools to study complex biological systems (Chaouiya *et al.* 2004; Montagud *et al.* 2019).
94 Logical modelling presents a qualitative approach consisting of modelling regulatory
95 networks using logical statements and allows for qualitative descriptions of dysregulated
96 cellular signalling cascades resulting from altered microenvironments (Albert and Thakar.
97 2014; Naldi *et al.* 2015; Thieffry. 2007). Within this formalism, interesting insights between
98 network structures and corresponding dynamical properties have been demonstrated
99 (Remy and Ruet. 2008).

100 Enciso *et al.* (2016) published a logical model focusing on the inflammatory BM
101 environment in response to TLR activation to capture NFK β -dependent inflammation
102 through disruption of the CXCL12/CXCR4 and VLA4/VCAM1 axis, accountable for the
103 onset of acute lymphoblastic leukaemia. We have elaborated upon this existing model to
104 produce an extended model that captures the crosstalk and the key signalling pathways
105 in the BM microenvironment whose alterations may lead to the onset of PMF.

106

107 **Methods**

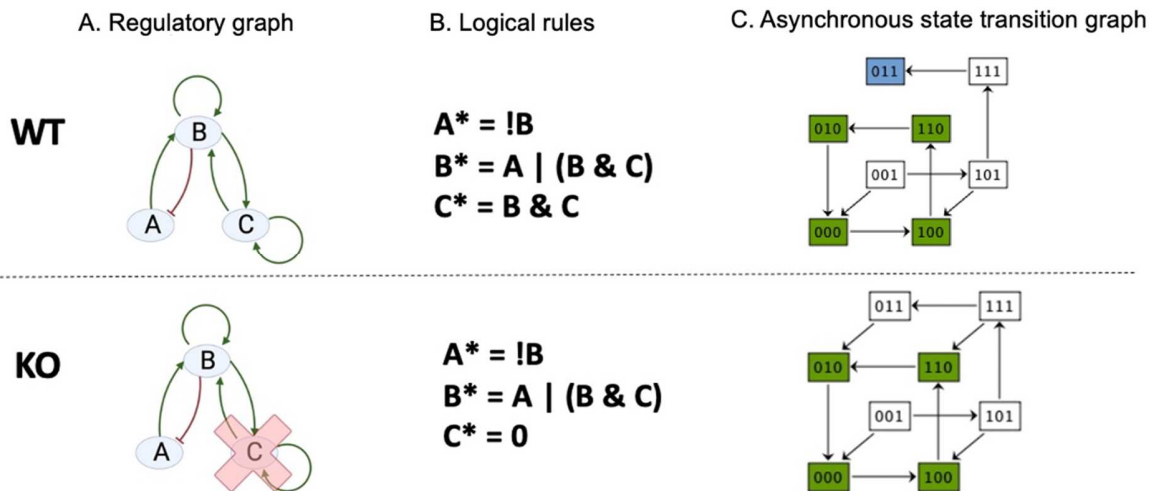
108 **Logical Modelling**

109 Logical modelling is a qualitative formalism developed to study the dynamics of complex
110 biological networks (Albert and Thakar. 2014; Abou-Jaoudé *et al.* 2016). Biological

111 information is extracted from the literature and/or experiments and abstracted into a
112 regulatory graph (RG), a directed signed graph whose nodes represent selected
113 biological species, connected by regulatory edges (positive edges for activations,
114 negative for inhibitions). Input nodes (nodes with only outgoing interactions) usually
115 represent the environment of the cell or any extracellular signal, and output nodes (that
116 only have incoming interactions and thus no impact on the model) usually serve as a
117 readout of the model. Outputs can reflect an observed phenotype such as 'proliferation'
118 and/or 'migration', as examples.

119 To introduce the dynamics, each node is associated with a discrete variable, denoting its
120 state (in the binary case, 0 (inactive) or 1 (active)). Nodes can also be assigned with
121 multivalued values that precise different thresholds, or activation levels. The global state
122 of the network is represented by a vector of n elements, where n represents the number
123 of nodes in the network. Each node is associated with logical rules that describe the target
124 value of the variable with respect to the state of the regulators of the node. These logical
125 rules set the dynamics and the asynchronous updating strategy provides non-
126 deterministic dynamics by updating a single component at each step. Trajectories
127 ultimately end within an attractor, i.e., terminal strongly connected component of the
128 graph and represent the asymptotic behaviours of the system. They can either be fixed
129 points (attractors of size one), or cyclical attractors (**Figure 1**).

130 Simulations of mutants consist of modifying the logical rules. Knock-out (KO) mutants are
131 simulated by blocking the logical rule of the desired node to 0, and Knock-in (KI) mutants
132 by fixing it to its maximal level or active at the desired threshold for multivalued nodes
133 (overexpression).



134

135 **Figure 1.** Toy model illustrating the logical modelling methodology. The first row depicts a wildtype (WT)
 136 situation, and the bottom row depicts a KO mutation of node C. **A)** The regulatory graph (RG) consists of 3
 137 nodes, A, B and C, and 6 edges, 5 activatory edges (green arrows) and one inhibitory edge (the red arrow).
 138 **B)** Logical rules are applied to each arc ('&' = 'and'; '|' = 'or'; '!' = 'not'),(*indicates possible future active
 139 state when the following logical rules are met). When node C has been knocked out (mutant version), its
 140 rule is blocked to 0. **C)** Asynchronous State Transition Graphs (STG). The asynchronous STG contains two
 141 attractors, a single fixed point [ABC] = [011] (coloured blue) and a cyclic attractor composed of the states
 142 {[000]; [100]; [110]; [010]} (coloured green). Asynchronous dynamics of the mutant C KO loses the fixed
 143 point and only results in the same cyclic attractor (coloured green).

144

145 The logical model was built using GINsim software and is available in XML format
 146 (GINML) on the GINsim Repository (<http://ginsim.org/node/253>, also provided in
 147 Supplementary File 1). All attractors belonging to either the wildtype and mutant
 148 simulations (double mutation JAK_H KI and JAK_MK KI) were sought and characterised
 149 using GINsim in conjunction with the CoLoMoTo toolbox (Levy *et al.* 2018) using Python.

150

151 Feedback Circuit Analysis

152 Feedback circuits are known to play a major role in the control of cell signalling dynamics.

153 For instance, the Thomas' rules state that the presence of positive (resp. negative) circuits

154 are necessary prerequisites to generate multistability (resp. sustained oscillations)
155 (Thomas. 1981; Thieffry. 2007).

156 When embedded within a RG, a circuit is regulated by some external nodes and thereby
157 its activity is affected. Circuit functionality contexts indicate the part of the space in which
158 the positive (resp. negative) circuit is able to generate local multistability (resp.
159 oscillations), and we say that the circuit is functional. These contexts are defined in terms
160 of constraints on the values of external nodes. The “Analyse circuits” tool of GINsim lists
161 all the functional circuits present in a logical model and their context of functionality.

162

163 MaBoSS Simulations

164 MaBoSS (Markovian Boolean Stochastic Simulator; Stoll *et al.* 2017) provides an
165 environment for simulating continuous/discrete time Markov processes based on logical
166 networks by applying the Gillespie algorithm. MaBoSS calculates the time evolution of
167 the probability of node states being activated and so was used to see if the model could
168 predict the probable onset of PMF with, and without JAK mutation as a means of model
169 validation. In addition, global and semi-global characterizations of the whole system are
170 computed. Simulation parameters involve running 50,000 simulations performed to
171 compute statistics and the maximum time representing the duration of the trajectory was
172 set to 30. For wildtype simulations, the initial states of all nodes were set to zero, apart
173 from the inputs; which were both set to be 100% active. The inputs for the JAK mutated
174 simulations account for TLR which was 100% probable of being activated. The initial
175 states of non-input nodes were then set to inactive apart from 'JAK_MK' and 'JAK_HSC',

176 as these were ectopically mutated to their maximum levels. The average temporal
177 evolution of selected nodes of the model were then plotted.

178

179 Results

180 Logical modelling of the bone marrow microenvironment and stem 181 cell crosstalk

182 A published logical model centred on the haematopoietic microenvironment between the
183 HSC and MSC explaining acute lymphoblastic leukaemia (Enciso *et al.* 2016) was used
184 as a starting model. This model which contains 26 nodes and 80 interactions,
185 encompasses the main communication pathways between HSC and MSC within the BM,
186 namely through CXCL12/CXCR4 and VLA4/VCAM1 signalling. Whilst keeping with TLR
187 signalling as an input, we replaced the original connexin43 input with TPO signalling due
188 to its relevance in PMF. We also extended the HSC submodel by including JAK-STAT
189 signalling pathway that is activated by either the TPO ligand or IL6 cytokine (Hasselbalch.
190 2013; Desterke *et al.* 2015; Fisher *et al.* 2019) which induces downstream PI3K/Akt
191 signalling pathways (DelaRosa and Lombardo. 2010; Kawai and Akira. 2007; Bartalucci
192 *et al.* 2013) and GCSF signalling (Schuettpelez *et al.* 2014; Brenner and Bruserud. 2019).
193 We also removed the nodes CXCR7 and GFIL1 from the original HSC submodel as these
194 nodes, despite being important in ALL, were considered to play a less important role in
195 the development of PMF. Additionally, we have expanded the initial model by including
196 an MK submodel, along with the main MK signalling pathways that are known to be
197 dysregulated in PMF, that is with JAK-STAT signaling (Coltro *et al.* 2021), TGF β (Malara

198 *et al.* 2018) and PF4 (Gleitz *et al.* 2020) production. Dysregulations in these pathways
199 have been observed to alter the crosstalk between HSC and MSCs in the context of PMF.

200 We then set the output of the model as 'PMF' and included two pseudo-output nodes,
201 'HSC_proliferation' and 'HSC_migration' that act as model readouts by concising
202 characteristic cell fates relating to the disease.

203 A further defining feature of the model is that we have made use of multivalued nodes to
204 discretise node activation states. Multivalued variables were associated with 9 nodes
205 which allowed the capture of several threshold effects related to those nodes. The JAK,
206 STAT, PI3K/Akt and NFK β nodes of the HSC and MK submodels were given multivalued
207 nodes. This is because 90% of PMF cases observe hyperactive JAK activity, resulting in
208 the overactivation of downstream STAT, PI3K/Akt and NFK β signalling within the HSC
209 submodel (Rumi *et al.* 2006). We were able to capture these threshold effects within the
210 model by allowing STAT, PI3K/Akt and NFK β nodes to take their activity from the
211 respective JAK activity, both in HSC and MK. The remaining node to be given a
212 multivalued threshold was 'HSC_proliferation' which takes its value from HSC PI3K/Akt
213 activity. HSC PI3K/Akt activity of 1 would activate 'HSC_proliferation' at its first, or basal
214 level (considered as normal behaviour for stem cells); whilst HSC PI3K/Akt at its
215 maximum threshold of 2 would then activate 'HSC_proliferation' at its highest level of 2.
216 This second threshold reflects hyperproliferation as a consequence of overactive
217 PI3K/Akt signalling, and this is associated with myeloproliferation (Skoda *et al.* 2015;
218 Fisher *et al.* 2021) which is associated with PMF. In this way, we could set the output of
219 the model as PMF, which is only activated when 'HSC_proliferation' has reached its
220 maximum level of 2, and when 'HSC_migration' and 'TGF β _MK' are activated.

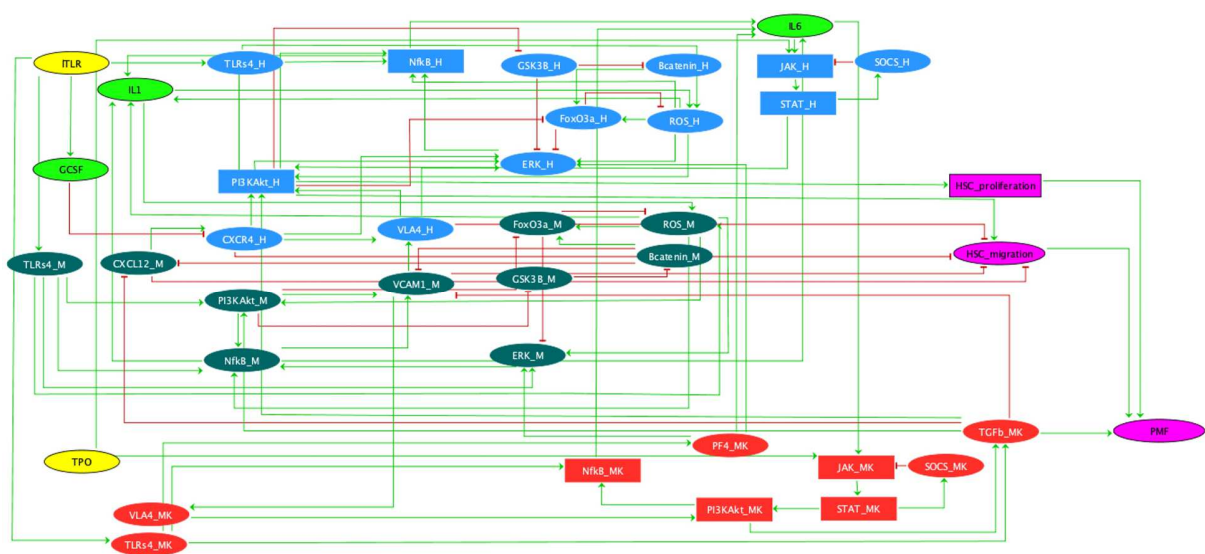
221 The central axis within this expanded model is the CXCL12/CXCR4 chemokine pathway
222 that now connects the MSC with HSC and MK submodels and plays essential roles in
223 homeostasis and haematopoiesis (Moll and Ransohoff. 2010; Tamura *et al.* 2011).
224 CXCR4 activation increases the affinity between VCAM1 expressed on the surface of
225 MSC and its receptor VLA4, expressed by HSCs and MKs. Both pathways,
226 CXCL12/CXCR4 and VCAM1/VLA4 are implicated with HSC migration (Lubkova *et al.*
227 2011; Moll and Ransohoff. 2010), and so the node 'HSC_migration' becomes activated
228 when either the CXCL12/CXCR4 or VCAM1/VLA4 communication axis are broken.
229 Otherwise, communication along these pathways triggers the PI3K/Akt and ERK
230 signalling pathways that govern cellular activity and physiology (Yu and Cui. 2016).

231 Recent evidence links elevated secretion of pro-inflammatory cytokines within the BM
232 niche in patients with PMF, including IL1 and IL6 (Desterke *et al.* 2015; Hasselbalch.
233 2013; Skoda *et al.* 2015), PF4 (Gleitz *et al.* 2020; Melo-Cardenas *et al.* 2021) and TGF β
234 (Agarwal *et al.* 2016; Yao *et al.* 2019). IL1 provides an amplification role with chronic
235 inflammation by activating PI3K/Akt and then NFK β signalling, resulting in elevated
236 production of both IL1, and ROS with the latter being counterbalanced by activation of
237 FOXO transcription factors (Naka *et al.* 2008; Zhang *et al.* 2016). At the mesenchymal
238 counterpart, TGF β being produced by the MK has been reported to inhibit both VCAM1
239 (Park *et al.* 2000) and CXCL12 (Chagraoui *et al.* 2002), yet upregulates ERK signalling
240 (Xue *et al.* 2020) and these interactions were also captured within the model. The
241 inclusion of GSK3 β and β -catenin in both HSC and MSC sub-models is relevant due to
242 their roles as intermediates of signalling transduction and regulation of the main
243 intracellular communication elements proposed in our network reconstruction.

244 Modifying and expanding the model (Enciso *et al.* 2016) in order to account for
 245 myelofibrotic conditioning of the BM microenvironment (based on evidence in the
 246 literature, see Methods), we have obtained an extended model containing 40 nodes and
 247 104 interactions (**Figure 2**).

248 This model was converted to a dynamical model by associating distinct logical rules to
 249 each node specifying the effect of the combination of the incoming interactions, based on
 250 biological knowledge. All logical rules and associated references can be found in
 251 **Supplementary Table S1**.

252 The model is available in XML format (GINML) on the GINsim Repository
 253 (<http://ginsim.org/node/253>).



254 **Figure 2.** Regulatory graph capturing the crosstalk between HSC (blue nodes), MSC (dark green nodes),
 255 MK (red nodes) and inflammatory cytokines (light green nodes) belonging to the BM microenvironment.
 256 Nodes are connected by directed edges representing activations (green) and inhibitions (red). Regardless
 257 of sub-model specificity, ellipse-shaped nodes represent Boolean nodes whilst rectangle-shaped nodes
 258 represent multivalued nodes. All logical rules and associated references can be found in Supplementary
 259 Table S1.

260

261 The topology of the regulatory graph consists of a unique strongly connected component
262 containing seven positive, and five negative functional circuits (see **Supplementary**
263 **Table S2**, and **Supplementary Figure S3**). Some of these functional circuits interconnect
264 all the cell submodels (HSC, MSC and MK), through the inflammatory cytokines submodel
265 which implies an important role of inflammatory cytokines associated with disease onset.
266 This emphasises that the cellular crosstalk between the several constituents of the BM
267 microenvironment is altered during the onset of PMF.

268

269 Wildtype Attractor Analysis predicts TLR and TPO stimulation drive 270 disease onset

271 We first investigated the attractors that describe the asymptotic behaviour of the model
272 for wildtype simulations (without any mutation). For each combination of inputs,
273 simulations resulted in a unique cyclic attractor. One cyclic attractor reveals a healthy
274 phenotype in which PMF is averted (inputs [TPO, TLR] = [0, 0]). Another predicts a
275 phenotype where the activity of the 'PMF' output oscillates between an active and inactive
276 state (inputs [TPO, TLR] = [1, 1]), which reflects potential disease onset. Intermediate
277 phenotypes are also observed in which the multivalued 'HSC_proliferation' and
278 'HSC_migration' nodes oscillate between inactive and active states, yet the remaining
279 outputs are inactive (inputs [TPO, TLR] = [0, 1]). Finally, a phenotype involving the
280 oscillation of the 'HSC_proliferation' node through all its states (0, 1 and 2), is observed

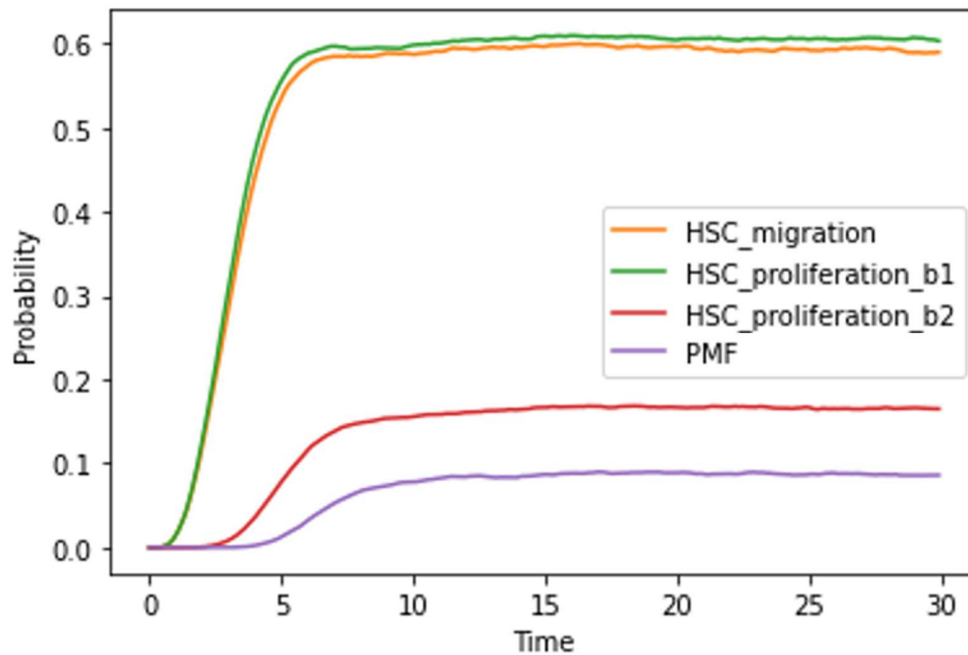
297 which then allows for a greater oscillatory nature of STAT and PI3K/Akt signalling which
298 activates 'HSC_proliferation'. This prediction is widely agreed and reported in literature,
299 (Panteli & Hatzmichael (2005); Hasselbalch (2013); Čokić et al., (2015); Fisher et al.,
300 2021). In this condition, 'TGFβ_MK' and 'PF4_MK' are both inactive and so the model
301 predicts that sole introduction of TPO input exerts a minor contribution to inflammation.

302 The presence of the TLR as a sole input triggers the activation of several positive
303 feedback circuits that impact the HSC, MSC, MK and BM microenvironment. One of these
304 cycles involves the direct activation of NFKβ and PI3K/Akt nodes from within the HSC
305 and MK submodels resulting in the activity of 'HSC_migration' to oscillate. This is because
306 TLR stimulates GCSF production (Schuettpelez et al., 2013, 2014) which contributes to
307 the inhibition of CXCR4 expression, as also observed by Kim et al., (2006) and Zhao et
308 al., (2020). TLR signalling also activates feedback cycles within the MK submodel that
309 involve PI3K/Akt activation. PI3K/Akt activated at its maximal level results in the
310 production of TGFβ from the MK which inhibits CXCL12 expression, yet upregulates
311 PI3K/Akt signalling within the HSC which activates 'HSC_migration. When 'PI3K/Akt_MK'
312 is inactive or at its basal level of 1, TGFβ is inactive and so CXCL12 remains activated
313 and allows communication with the MSC via CXCR4.

314 When both inputs are introduced, we observe oscillations of the 'PMF' output and so this
315 attractor may describe a subset of PMF patients who don't exhibit any driver mutation
316 which may agree with the clinical data (Agarwal *et al.* 2016). In addition, TPO and TLR
317 activate negative feedback circuits which result in the oscillatory activation of the
318 'HSC_migration' node. This cyclic attractor represents the communication breakdown of
319 the HSC with the MSC and its migration out of the BM, as a result of TGFβ production. It

320 is only in situations where the oscillatory activity of 'HSC_proliferation' is at its maximal
321 level, and when the HSC is migrating, that we see the activation of the output node 'PMF'.
322 On the contrary, the onset of PMF is predicted to be avoided when the oscillatory activity
323 of TGF β remains inactive and when the HSC PI3K/Akt pathway remains in a status that
324 is below its maximal activity.

325 In order to get a finer description of the attractors, we ran stochastic simulations using
326 MaBoSS (see methods). In particular, we wanted to calculate the probability of the 'PMF'
327 output node being activated within the cyclic attractor obtained with both inputs present.
328 As MaBoSS considers only Boolean systems, the multivalued node HSC_proliferation
329 has been duplicated in two Boolean nodes, 'HSC_proliferation_b1' (centred on the
330 threshold 1) and 'HSC_proliferation_b2' (centred on the threshold 2). When [TPO, TLR]
331 = [1, 1], we observe that the nodes 'HSC_migration' and 'HSC_proliferation_b1' follow
332 similar trajectories and both have a 55-60% probability of being activated in this cyclic
333 attractor. The probability of 'HSC_proliferation_b2' node ('HSC_proliferation' at its
334 maximum level of 2) being activated in these conditions was predicted to happen with
335 17% probability, whilst activation of the 'PMF' output node was predicted to be activated
336 with a probability of 8% which agrees with clinical data that 7-10% of PMF patients test
337 negative for any of the driver mutations that overactive JAK signaling (**Figure 4**). We also
338 investigated the probability of the oscillatory nodes JAK and TGF β being activated in the
339 cyclic attractor (**Figure 5**).

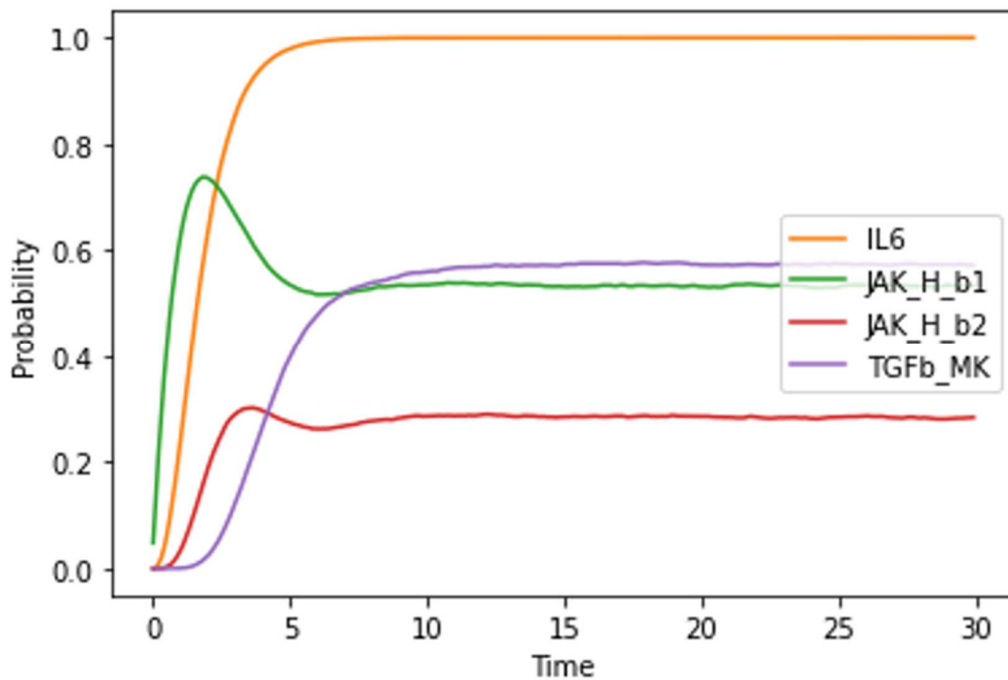


340

341 **Figure 4.** Probability of output nodes to be activated in the cyclic attractor from MaBoSS WT simulations,
 342 with both inputs present. 'HSC_proliferation_b1' represents the node has reached level 1 and
 343 'HSC_proliferation_b2' is when the node has reached level 2.

344

345 MaBoSS simulations showed an early increase in JAK activity, with the probability of
 346 being active at level 1 stabilising at 55% (after a transient peak at 70%). The probability
 347 of JAK achieving its level 2 activation is observed to be 30%. Once activated, 'JAK_H'
 348 remains activated because of sustained activation of IL6 which overrides the negative
 349 cycle involving SOCS inhibition of JAK. TGF β release from MK was estimated to be 55%
 350 probable (**Figure 5**).



351

352 **Figure 5.** Probability of select nodes to be activated in the cyclic attractor from MaBoSS WT simulations,
 353 in the presence of both inputs. 'JAK_H_b1' represents the node reaching level 1 and 'JAK_H_b2' is when
 354 this multivalued node has reached level 2.

355

356 When comparing **Figures 4** and **5**, we observe a concomitant activation of HSC migration
 357 and proliferation (at level 1) with the progressive increase of IL6 activation and the
 358 probability of activating 'JAK_H' at its highest level is also increasing. This might explain
 359 the increase in probable activation of HSC over proliferation ('HSC_proliferation_b2').
 360 Meanwhile, the probability of TGFβ release increases, which explains the increasing
 361 probability of activating PMF. The prediction regarding the oscillatory dynamics of TGFβ
 362 has been well documented in the literature (see Zi et al., (2012) and has also been
 363 associated to fibrosis (Dewidar et al., 2019), serving as other model validations.

364

365

366 To conclude, these simulations reveal that in the absence of the JAK mutation (WT
367 situation), both inputs TPO and TLR have to be present for PMF to be activated, probably
368 arising from a JAK overactivation which cascades inflammatory feedback circuits through
369 IL6 and TGF β pathways. Activation of TPO alone exerts a minor contribution to
370 inflammation without the presence of the JAK mutation.

371 **Jak Mutated Analysis predicts the presence of TLR alone is**
372 **sufficient to drive disease onset**

373 All known driver mutations associated with PMF induce overactive JAK activity and
374 downstream STAT signalling, and are observed in 90% of PMF cases, whilst 0.1 - 0.2%
375 of the population harbour the JAK mutation but do not display signs of the disease
376 (Agarwal *et al.* 2016). In an attempt to explain why some patients with the overactive JAK
377 activity eventually manifest with PMF whilst others do not, we simulated 'JAK_H' and
378 'JAK_MK' KI mutants. In this scenario, the model displays 4 fixed points, one per
379 combination of input nodes (**Figure 6**). These fixed points reveal two healthy phenotypes
380 (inputs [TPO, TLR] = [0, 0]; [1, 0]), and two that activate PMF (inputs [TPO, TLR] = [0, 1];
381 [1, 1]).

399 the effect of maintaining communication between the HSC and MSC via both the VCAM/VLA4
400 and CXCL12/CXCR4 mediated crosstalk. As expected, MABOSS reveals that the probability of
401 'HSC_migration' to be activated is 0%, yet 'HSC_proliferation' is activated with a probability of
402 100% (Supplementary Figure S4). As such, we can evaluate the contribution of TPO signalling to
403 exert a minor effect with myelofibrosis, when introduced as a sole input in the presence of JAK
404 mutation. As such, we can evaluate the contribution of TPO signalling to exert a minor
405 effect with myelofibrosis, when introduced as a sole input in the presence of JAK mutation.

406

407 Following activation of both inputs for JAK mutated simulations, TLR signalling augments
408 the JAK burden in the MK submodel causing overactivation of PI3K/Akt signalling and
409 this time, NFK β signalling. TPO also augments JAK stimulation, and TLR activates GCSF
410 and PF4, and inactivates CXCR4 and VLA4, resulting in the loss of communication
411 between the HSC and MSC submodels. Hyperactive JAK signalling within the HSC
412 submodel led to overactive PI3K/Akt, and when combined with the activation of
413 'HSC_migration' and TGF β , led to the activation of the output node 'PMF', at a calculated
414 probability of 100% (**Supplementary Figure S5**).

415 Again, these results agree with the literature that shows activation of TPO and JAK are
416 both required to induce a myelofibrotic phenotype (Besancenot *et al.* 2014). Furthermore,
417 PF4 (Gleitz *et al.* 2020) and TGF β (Chagraoui *et al.* 2002; Zingariello *et al.* 2013; Agarwal
418 *et al.* 2016) are critically implicated with disease progression. In conclusion, JAK (KI)
419 mutated simulations predict that TLR signalling is sufficient to perturb the
420 microenvironment and disrupt HSC-MSC crosstalk to drive disease onset.

421

422 Discussion and Conclusion

423 Primary myelofibrosis is an untreatable age-related disorder of haematopoiesis in which
424 a break in the crosstalk between progenitor HSCs and neighbouring mesenchymal stem
425 cells (MSC) caused HSCs to rapidly proliferate and migrate out of the bone marrow. In
426 this work, we have elaborated and adapted a pre-existing logical model of lymphoblastic
427 leukaemia (Encisco et al., 2016) to account for the BM microenvironment with the primary
428 aim of capturing stem cell cross-talk between HSC, MSC and megakaryocyte progenitors.
429 We then used the model to capture the dysregulation of the cell crosstalk following
430 perturbation of the BM microenvironment due to stimulation with TPO, and/or activation
431 of TLR, for wildtype and in ectopically JAK mutated situations. We chose to include TPO
432 and TLR signalling as inputs due to their roles in mediating chronic inflammation.

433 The model predicted that for wildtype scenarios, the presence of both inputs (TPO and
434 TLR) resulted in a probability of disease. TLR signalling was predicted to activate PF4,
435 which agrees with (Gleitz *et al.* 2020) who report that elevated expression of PF4 links
436 inflammation with progression of BM fibrosis. The authors also report that the absence of
437 PF4 reduces the extent of BM remodelling in presence of overactive JAK pathways, which
438 our model has qualitatively captured (**Figure 3; Figure 6**). Our results suggest that TLR
439 signalling cascades positive and negative feedback circuits that are responsible for
440 triggering an initial event of chronic inflammation through the activation of PF4 and TGF β .
441 TPO signalling cascaded further positive and negative feedback circuits that facilitate
442 HSC hyperproliferation, independent of the JAK mutation. These predictions might
443 explain why patients who test negative for the JAK mutation can still be diagnosed with

444 PMF, in which continual exposure to TPO and TLR receptor activation may trigger the
445 onset of PMF. Oscillations in the activity levels of several biological actors are known to play
446 important roles in cell signaling. Positive feedback circuits, acting on their own or in combination
447 with negative feedback circuits are a common feature of oscillating biological systems
448 (Kholodenko, B.N., 2006). Interestingly, all JAK WT simulations resulting with certain nodes
449 whose activity level oscillates and which then determine cyclic attractors being obtained nodes.
450 PI3K/Akt activity and its downstream effectors are known to be dynamically regulated in response
451 to specific stimuli, such as growth factors, hormones, or cellular stress. This regulation further
452 exhibits temporal dynamics characterized by rapid activation followed by gradual deactivation as
453 the cells respond to the external stimuli and adapt to the changing environment (Madsen &
454 Vanhaesebroeck., 2020). The model has predicted an oscillating activity of PI3K/Akt nodes
455 associated to the HSC and MK submodels in all 4 combinations of inputs (Figure 3), and as such
456 results in oscillating activity of NFK β . NFK β is a well-studied transcription factor that displays
457 intrinsic oscillatory behavior (see Nelson et al., 2004) and plays a prominent role in inflammation
458 attributed to many diseases including PMF (Gangat, N., & Tefferi, A., 2020). As seen in Figure 3,
459 the model has predicted an oscillation of the NFK β node associated to the HSC and MK
460 submodels for WT simulations when TLR and TPO are both introduced as inputs, in agreement
461 with the experimental evidence. There is also, in the same cyclic attractor, an oscillation
462 associated to MSC CXCL12 node (Figure 3). There is currently limited work specifically
463 addressing the oscillation of CXCL12 in myelofibrosis despite CXCL12 and its receptor CXCR4
464 play a clear role in the pathogenesis of the disease. In myelofibrosis, the bone marrow
465 microenvironment undergoes significant changes, including alterations in cytokine and
466 chemokine expression. Further research is therefore needed to better understand the role of
467 CXCL12 in myelofibrosis and to determine whether it presents oscillatory patterns or dynamic
468 changes in expression levels over time.

469 JAK mutated (KI) simulations revealed that TLR alone was sufficient to drive
470 myelofibrosis. The model also predicted that in the presence of JAK mutation and
471 absence of TLR, PMF was averted which supports the observation that 0.1 – 0.2% of the
472 general population harbour the JAK mutation without showing overt signs of any
473 myeloproliferative disease (**Figure 6**). We hypothesise that the probability of TLR and
474 TPO signalling increases with time, explaining why the onset of PMF is age-related.

475 Mathematical modelling aims at abstracting and understanding the effects of biological
476 perturbations to suggest ways to intervene and re-establish homeostasis. This is
477 challenging to achieve within any modelling framework. The model presented in this work
478 contains limited, but sufficient biological interactions that play a role in the onset of PMF.
479 We sought to capture as much information as possible while maintaining enough
480 abstraction to obtain a manageable model of reasonable size for the analysis to be
481 performed. This has allowed the construction of a model that agrees qualitatively -and in
482 some respects even quantitatively- with experimental and clinical data. As a limitation, we
483 are modelling the crosstalk between single cells, while in reality, multiple cells reside
484 within a niche which our approach does not take into account. It is therefore essential to
485 explore the dynamics at the scale of interacting cell populations, taking into account their
486 response, death and interactions. This requires a proper computational description of
487 heterogeneous interacting cell populations, and this model could be the basis of such
488 modelling at the cell population level microenvironment.

489 In conclusion, we have built an intra- and intercellular logical model that is able to capture
490 the crosstalk between distinct progenitor stem cells within the BM microenvironment. The
491 model is able to predict and explain the onset of myelofibrosis for JAK-positive and JAK-

492 negative cases. More generally, this model could be useful for the study of other
493 haematopoietic diseases.

494

495 **Declarations**

496 **Ethics approval and consent to participate**

497 Not applicable
498

499 **Consent for publication**

500 Not applicable
501

502 **Data availability**

503 The data underlying this article are available within the GINsim repository at

504 <http://ginsim.org/node/253>
505

506 **Declaration of interest**

507 Declaration of interest: none
508

509 **Funding**

510 ED laboratory is supported by the Ligue Nationale Contre le Cancer, This work has been
511 supported by the the Fondation A*MIDEX.

512 Authors contributions

513 ED thought up and designed this work. ER supervised the modelling methodology. SC built, ran
514 and analysed the model and wrote the manuscript. All authors read and approved the final
515 article.

516

517 Acknowledgements

518 The authors would like to thank A. Naldi for his assistance with GINsim, P. Monteiro for
519 uploading the model to the GINsim model repository, F. Zaccagnino for assisting with
520 MaBoSS and B. Habermann for proofreading the manuscript.

521 References

522 Abou-Jaoudé W, Traynard P, Monteiro PT, Saez-Rodriguez J, Helikar T, Thieffry D,
523 Chaouiya C. Logical modeling and dynamical analysis of cellular networks. *Frontiers in*
524 *genetics*. 2016 May 31;7:94.

525 Agarwal A, Morrone K, Bartenstein M, Zhao ZJ, Verma A, Goel S. Bone marrow fibrosis
526 in primary myelofibrosis: pathogenic mechanisms and the role of TGF- β . *Stem cell*
527 *investigation*. 2016;3.

528 Albert R, Thakar J. Boolean modeling: a logic-based dynamic approach for understanding
529 signaling and regulatory networks and for making useful predictions. *Wiley*
530 *Interdisciplinary Reviews: Systems Biology and Medicine*. 2014 Sep;6(5):353-69.

531 Bartalucci N, Guglielmelli P, Vannucchi AM. Rationale for targeting the PI3K/Akt/mTOR
532 pathway in myeloproliferative neoplasms. *Clinical Lymphoma Myeloma and Leukemia*.
533 2013 Sep 1;13:S307-9.

534 Bartels S, Faisal M, Büsche G, Schlue J, Hasemeier B, Schipper E, Vogtmann J,
535 Westphal L, Lehmann U, Kreipe H. Mutations associated with age-related clonal
536 hematopoiesis in PMF patients with rapid progression to myelofibrosis. *Leukemia*. 2020
537 May;34(5):1364-72.

538 Besancenot R, Roos-Weil D, Tonetti C, Abdelouahab H, Lacout C, Pasquier F, Willekens
539 C, Rameau P, Lecluse Y, Micol JB, Constantinescu SN. JAK2 and MPL protein levels
540 determine TPO-induced megakaryocyte proliferation vs differentiation. *Blood, The*
541 *Journal of the American Society of Hematology*. 2014 Sep 25;124(13):2104-15.

- 542 Brenner AK, Bruserud Ø. Functional toll-like receptors (TLRs) are expressed by a majority
543 of primary human acute myeloid leukemia cells and inducibility of the TLR signaling
544 pathway is associated with a more favorable phenotype. *Cancers*. 2019 Jul 11;11(7):973.
- 545 Caocci, G., Greco, M., & La Nasa, G. (2017). Bone marrow homing and engraftment
546 defects of human hematopoietic stem and progenitor cells. *Mediterranean journal of*
547 *hematology and infectious diseases*, 9(1).
- 548 Chagraoui H, Komura E, Tulliez M, Giraudier S, Vainchenker W, Wendling F. Prominent
549 role of TGF- β 1 in thrombopoietin-induced myelofibrosis in mice. *Blood, The Journal of*
550 *the American Society of Hematology*. 2002 Nov 15;100(10):3495-503.
- 551 Chaouiya, C., Remy, E., Ruet, P., & Thieffry, D. (2004, June). Qualitative modelling of
552 genetic networks: From logical regulatory graphs to standard petri nets. In *International*
553 *Conference on Application and Theory of Petri Nets* (pp. 137-156). Springer, Berlin,
554 Heidelberg.
- 555 Čokić, V. P., Mitrović-Ajtić, O., Beleslin-Čokić, B. B., Marković, D., Buač, M., Diklić, M., ...
556 & Raj, P. K. (2015). Proinflammatory cytokine IL-6 and JAK-STAT signaling pathway in
557 myeloproliferative neoplasms. *Mediators of inflammation*, 2015.
- 558 Coltro G, Loscocco GG, Vannucchi AM. Classical Philadelphia-negative
559 myeloproliferative neoplasms (MPNs): A continuum of different disease entities.
560 *International Review of Cell and Molecular Biology*. 2021 Jan 1;365:1-69.
- 561 Cornish-Bowden A, Cárdenas ML. Self-organization at the origin of life. *Journal of*
562 *theoretical biology*. 2008 Jun 7;252(3):411-8.
- 563 Cui L, Moraga I, Lerbs T, Van Neste C, Wilmes S, Tsutsumi N, Trotman-Grant AC,
564 Gakovic M, Andrews S, Gotlib J, Darmanis S. Tuning MPL signaling to influence
565 hematopoietic stem cell differentiation and inhibit essential thrombocythemia progenitors.
566 *Proceedings of the National Academy of Sciences*. 2021 Jan 12;118(2):e2017849118.
- 567 DelaRosa O, Lombardo E. Modulation of adult mesenchymal stem cells activity by toll-
568 like receptors: implications on therapeutic potential. *Mediators of inflammation*. 2010.
- 569 Desterke C, Martinaud C, Ruzehaji N, Bousse-Kerdilès L. Inflammation as a keystone of
570 bone marrow stroma alterations in primary myelofibrosis. *Mediators of inflammation*.
571 2015.
- 572 Dewidar, B., Meyer, C., Dooley, S., & Meindl-Beinker, N. (2019). TGF- β in hepatic stellate
573 cell activation and liver fibrogenesis—updated 2019. *Cells*, 8(11), 1419.
- 574 Enciso, J., Mayani, H., Mendoza, L., & Pelayo, R. (2016). Modeling the pro-inflammatory
575 tumor microenvironment in acute lymphoblastic leukemia predicts a breakdown of
576 hematopoietic-mesenchymal communication networks. *Frontiers in physiology*, 7, 349.

- 577 Fisher DA, Miner C, Engle E, Collins TB, Hu H, Malkova O, Oh S. Mass Cytometry
578 Analysis Reveals Cellular Loci of Cytokine Overproduction in Myelofibrosis with
579 Differential Sensitivity to Ruxolitinib. *Blood*. 2017 Dec 8;130:4209.
- 580 Fisher DA, Miner CA, Engle EK, Hu H, Collins TB, Zhou A, Allen MJ, Malkova ON, Oh
581 ST. Cytokine production in myelofibrosis exhibits differential responsiveness to JAK-
582 STAT, MAP kinase, and NF κ B signaling. *Leukemia*. 2019 Aug;33(8):1978-95.
- 583 Fisher DA, Fowles JS, Zhou A, Oh, S. T. Inflammatory pathophysiology as a contributor
584 to myeloproliferative neoplasms. *Frontiers in immunology*. 2021 Jun 1;12:2034.
- 585 Gangat, N., & Tefferi, A. (2020). Myelofibrosis biology and contemporary management.
586 *British journal of haematology*, 191(2), 152-170.
- 587 Gleitz HF, Dugourd AJ, Leimkühler NB, Snoeren IA, Fuchs SN, Menzel S, Ziegler S,
588 Kröger N, Trivai I, Büsche G, Kreipe H. Increased CXCL4 expression in hematopoietic
589 cells links inflammation and progression of bone marrow fibrosis in MPN. *Blood*. 2020 Oct
590 29;136(18):2051-64.
- 591 Hasselbalch HC. The role of cytokines in the initiation and progression of myelofibrosis.
592 *Cytokine & growth factor reviews*. 2013 Apr 1;24(2):133-45.
- 593 Kawai T, Akira S. Signaling to NF- κ B by Toll-like receptors. *Trends in molecular medicine*.
594 2007 Nov 1;13(11):460-9.
- 595 Kim, H. K., De La Luz Sierra, M., Williams, C. K., Gulino, A. V., & Tosato, G. (2006). G-
596 CSF down-regulation of CXCR4 expression identified as a mechanism for mobilization of
597 myeloid cells. *Blood*, 108(3), 812-820.
- 598 Kholodenko, B. N. (2006). Cell-signalling dynamics in time and space. *Nature reviews*
599 *Molecular cell biology*, 7(3), 165-176.
- 600 Kuykendall AT, Horvat NP, Pandey G, Komrokji R, Reuther GW. Finding a Jill for JAK:
601 assessing past, present, and future JAK inhibitor combination approaches in
602 myelofibrosis. *Cancers*. 2020 Aug 14;12(8):2278.
- 603 Levy N, Naldi A, Hernandez C, Stoll G, Thieffry D, Zinovyev A, Calzone L, Paulevé L.
604 Prediction of mutations to control pathways enabling tumor cell invasion with the
605 CoLoMoTo interactive notebook (tutorial). *Frontiers in physiology*. 2018 Jul 6;9:787.
- 606 Liekens S, Schols D, Hatse S. CXCL12-CXCR4 axis in angiogenesis, metastasis and
607 stem cell mobilization. *Current pharmaceutical design*. 2010 Dec 1;16(35):3903-20.
- 608 Lubkova ON, Tzvetaeva NV, Momotyuk KS, Belkin VM, Manakova TE. VCAM-1
609 expression on bone marrow stromal cells from patients with myelodysplastic syndromes.
610 *Bulletin of experimental biology and medicine*. 2011 May;151(1):13-5.

- 611 Madsen, R. R., & Vanhaesebroeck, B. (2020). Cracking the context-specific PI3K
612 signaling code. *Science Signaling*, 13(613), eaay2940.
- 613 Malara A, Abbonante V, Zingariello M, Migliaccio A, Balduini A. Megakaryocyte
614 contribution to bone marrow fibrosis: many arrows in the quiver. *Mediterranean Journal*
615 *of Hematology and Infectious Diseases*. 2018;10(1).
- 616 Mascarenhas, J., Gleitz, H. F., Chifotides, H. T., Harrison, C. N., Verstovsek, S.,
617 Vannucchi, A. M., ... & List, A. F. (2022). Biological drivers of clinical phenotype in
618 myelofibrosis. *Leukemia*, 1-10.
- 619 Melo-Cardenas J, Migliaccio AR, Crispino JD. The role of megakaryocytes in
620 myelofibrosis. *Hematology/Oncology Clinics*. 2021 Apr 1;35(2):191-203.
- 621 Montagud, A., Traynard, P., Martignetti, L., Bonnet, E., Barillot, E., Zinovyev, A., &
622 Calzone, L. (2019). Conceptual and computational framework for logical modelling of
623 biological networks deregulated in diseases. *Briefings in bioinformatics*, 20(4), 1238-
624 1249.
- 625 Moll, N. M., & Ransohoff, R. M. (2010). CXCL12 and CXCR4 in bone marrow physiology.
626 *Expert review of hematology*, 3(3), 315-322.
- 627 Naka K, Muraguchi T, Hoshii T, Hirao A. Regulation of reactive oxygen species and
628 genomic stability in hematopoietic stem cells. *Antioxidants & redox signaling*. 2008 Nov
629 1;10(11):1883-94.
- 630 Naldi A, Monteiro PT, Müssel C, Consortium for Logical Models and Tools, Kestler HA,
631 Thieffry D, Xenarios I, Saez-Rodriguez J, Helikar T, Chaouiya C. Cooperative
632 development of logical modelling standards and tools with CoLoMoTo. *Bioinformatics*.
633 2015 Apr 1;31(7):1154-9.
- 634 Nelson, D. E., Ihekwaba, A. E. C., Elliott, M., Johnson, J. R., Gibney, C. A., Foreman, B.
635 E., ... & White, M. R. H. (2004). Oscillations in NF- κ B signaling control the dynamics of
636 gene expression. *Science*, 306(5696), 704-708.
- 637 Nielsen C, Bojesen SE, Nordestgaard BG, Kofoed KF, Birgens HS. JAK2V617F somatic
638 mutation in the general population: myeloproliferative neoplasm development and
639 progression rate. *haematologica*. 2014 Sep;99(9):1448.
- 640 Panteli, K. E., Hatzimichael, E. C., Bouranta, P. K., Katsaraki, A., Seferiadis, K., Stebbing,
641 J., & Bourantas, K. L. (2005). Serum interleukin (IL) α 1, IL α 2, sIL α 2Ra, IL α 6 and
642 thrombopoietin levels in patients with chronic myeloproliferative diseases. *British journal*
643 *of haematology*, 130(5), 709-715.
- 644 Pardanani A, Vannucchi AM, Passamonti F, Cervantes F, Barbui T, Tefferi A. JAK
645 inhibitor therapy for myelofibrosis: critical assessment of value and limitations. *Leukemia*.
646 2011 Feb;25(2):218-25.

- 647 Park SK, Yang WS, Lee SK, Ahn H, Park JS, Hwang O, Lee JD. TGF- β 1 down-regulates
648 inflammatory cytokine-induced VCAM-1 expression in cultured human glomerular
649 endothelial cells. *Nephrology Dialysis Transplantation*. 2000 May 1;15(5):596-604.
- 650 Qian H, Beard DA. Metabolic futile cycles and their functions: a systems analysis of
651 energy and control. *IEE Proceedings-Systems Biology*. 2006 Jul 1;153(4):192-200.
- 652 Remy E, Ruet P. From minimal signed circuits to the dynamics of Boolean regulatory
653 networks. *Bioinformatics*. 2008 Aug 15;24(16):i220-6.
- 654 Rumi E, Passamonti F, Pietra D, Porta MG, Arcaini L, Boggi S, Elena C, Boveri E,
655 Pascutto C, Lazzarino M, Cazzola M. JAK2 (V617F) as an acquired somatic mutation and
656 a secondary genetic event associated with disease progression in familial
657 myeloproliferative disorders. *Cancer: Interdisciplinary International Journal of the*
658 *American Cancer Society*. 2006 Nov 1;107(9):2206-11.
- 659 Rumi, E., Trotti, C., Vanni, D., Casetti, I. C., Pietra, D., & Sant'Antonio, E. (2020). The
660 genetic basis of primary myelofibrosis and its clinical relevance. *International Journal of*
661 *Molecular Sciences*, 21(23), 8885.
- 662 Schuettpelez LG, Borgerding JN, Christopher MJ, Gopalan PK, Romine MP, Herman AC,
663 Woloszynek JR, Greenbaum AM, Link DC. G-CSF regulates hematopoietic stem cell
664 activity, in part, through activation of Toll-like receptor signaling. *Leukemia*. 2014
665 Sep;28(9):1851-60.
- 666 Schuettpelez, L. G., & Link, D. C. (2013). Regulation of hematopoietic stem cell activity by
667 inflammation. *Frontiers in immunology*, 4, 204.
- 668 Skoda, R.C., Duek, A. and Grisouard, J., 2015. Pathogenesis of myeloproliferative
669 neoplasms. *Experimental hematology*, 43(8), pp.599-608.
- 670 Stark GR, Darnell Jr JE. The JAK-STAT pathway at twenty. *Immunity*. 2012 Apr
671 20;36(4):503-14.
- 672 Stoll G, Caron B, Viara E, Dugourd A, Zinovyev A, Naldi A, Kroemer G, Barillot E, Calzone
673 L. MaBoSS 2.0: an environment for stochastic Boolean modeling. *Bioinformatics*. 2017
674 Jul 15;33(14):2226-8.
- 675 Tamura M, Sato MM, Nashimoto M. Regulation of CXCL12 expression by canonical Wnt
676 signaling in bone marrow stromal cells. *The international journal of biochemistry & cell*
677 *biology*. 2011 May 1;43(5):760-7.
- 678 Tefferi A, Vannucchi AM. Genetic risk assessment in myeloproliferative neoplasms.
679 *In Mayo Clinic Proceedings* 2017 Aug 1 (Vol. 92, No. 8, pp. 1283-1290). Elsevier.
- 680 Thieffry D. Dynamical roles of biological regulatory circuits. *Briefings in bioinformatics*.
681 2007 Jul 1;8(4):220-5.

- 682 Thomas R. On the relation between the logical structure of systems and their ability to
683 generate multiple steady states or sustained oscillations. *Numerical methods in the study*
684 *of critical phenomena* 1981 (pp. 180-193). Springer, Berlin, Heidelberg.
- 685 Varghese LN, Defour JP, Pecquet C, Constantinescu SN. The thrombopoietin receptor:
686 structural basis of traffic and activation by ligand, mutations, agonists, and mutated
687 calreticulin. *Frontiers in endocrinology*. 2017 Mar 31;8:59.
- 688 Xue VW, Chung JY, Córdoba CA, Cheung AH, Kang W, Lam EW, Leung KT, To KF, Lan
689 HY, Tang PM. Transforming growth factor- β : a multifunctional regulator of cancer
690 immunity. *Cancers*. 2020 Oct 23;12(11):3099.
- 691 Yao JC, Abou Ezzi G, Krambs JR, Uttarwar S, Duncavage EJ, Link DC. TGF- β Signaling
692 Contributes to Myelofibrosis and Clonal Dominance of Myeloproliferative Neoplasms.
693 *Blood*. 2019 Nov 13;134:470.
- 694 Yu JS, Cui W. Proliferation, survival and metabolism: the role of PI3K/AKT/mTOR
695 signalling in pluripotency and cell fate determination. *Development*. 2016 Sep
696 1;143(17):3050-60.
- 697 Zhang J, Wang X, Vikash V, Ye Q, Wu D, Liu Y, Dong W. ROS and ROS-mediated cellular
698 signaling. *Oxidative medicine and cellular longevity*. 2016 Oct;2016.
- 699 Zhao, F. Y., Cheng, T. Y., Yang, L., Huang, Y. H., Li, C., Han, J. Z., ... & Liu, W. (2020).
700 G-CSF inhibits pulmonary fibrosis by promoting BMSC homing to the lungs via SDF-
701 1/CXCR4 chemotaxis. *Scientific Reports*, 10(1), 1-11.
- 702 Zi, Z., Chapnick, D. A., & Liu, X. (2012). Dynamics of TGF- β /Smad signaling. *FEBS*
703 *letters*, 586(14), 1921-1928.
- 704 Zingariello M, Martelli F, Ciaffoni F, Masiello F, Ghinassi B, D'Amore E, Massa M, Barosi
705 G, Sancillo L, Li X, Goldberg JD. Characterization of the TGF- β 1 signaling abnormalities
706 in the Gata1^{low} mouse model of myelofibrosis. *Blood*, *The Journal of the American*
707 *Society of Hematology*. 2013 Apr 25;121(17):3345-63.